Journal of Control, Automation and Electrical Systems (2024) 35:401–414
https://doi.org/10.1007/s40313-024-01066-0

Fluidization of Stochastic Petri Nets via Continuous Petri Nets: Comparative Study

Hamid El-Moumen[1] · **Nabil El Akchioui**[1]

Received: 8 September 2023 / Revised: 1 January 2024 / Accepted: 4 January 2024 / Published online: 6 February 2024

Abstract
Fluidization is a crucial technique for converting stochastic Petri nets (SPNs) into continuous Petri nets (CPNs) to overcome the challenge of combinatorial state explosion, which results in prolonged computational time for steady-state probability estimates. The ultimate aim is to obtain a precise continuous model that captures the behavior of the SPN. However, fluidization's continuous behavior is distinct from typical stochastic systems. In this study, we conducted an in-depth analysis of fluidization in single and multiple regions. We considered different approaches, including piecewise linear and adaptive techniques, and added sufficient conditions to both approaches to achieve superior convergence between the two models. Our results are interpreted and compared. The adaptive approach, which utilizes a nonlinear adaptive law to minimize errors caused by average throughput and average marking variations, achieved excellent convergence compared to the piecewise linear approach, which involves several steps, such as subdividing marking trajectories into multiple phases and intermediate points. Overall, this study highlights the effectiveness of the adaptive approach in enhancing convergence in CPNs.

Keywords Reliability analysis · Markov model · Combinatorial explosion · Stochastic Petri nets · Fluidization · Continuous Petri nets · Adaptive approach · Piecewise linear approach

1 Introduction

The decision-making process to ensure reliability is critical in both complex engineering systems, such as power plants, offshore oil platforms, chemical production factories, and public transportation networks, as well as in large-scale environments involving multiple stakeholders, such as water distribution networks, regional power grids, and railway and air transportation systems. Reliability analysis of intricate dynamical systems usually employs stochastic discrete event models like Markov models and stochastic Petri nets (SPNs) (Bobbio et al., 1998; El-Moumen et al., 2023). Consequently, it becomes imperative to tailor existing techniques and tools to suit the specificities of these systems. Nonetheless, conventional analytical methods, such as the Markov model (El Moumen et al., 2023b), are no longer viable for systems that comprise a multitude of interdependent components. The combinatorial explosion problem of state numbers in discrete event systems poses a significant challenge for reliability analysis and dynamic system synthesis (Pinto et al., 2021; Vázquez-Serrano et al., 2021). The exponential growth in the number of states results in a highly complex calculation of the marking graph for the Markov model, which in turn makes the Markov analysis impractical (Ribeiro et al., 2018). Instead, SPNs are used as an estimator for the Markov model (Vázquez et al., 2008). The main advantage of this estimator is that it eliminates the need to determine the marking graph required by the Markov model method (Kalaiarasi et al., 2017; Moumen et al., 2022). However, this approach results in a longer convergence time to reach steady-state probabilities (del Foyo & Silva, 2017; Moumen et al., 2022). In general, this phenomenon is because information throughput is discrete (Bobbio et al., 1998; Florin et al., 1991). Most solutions to this problem aim to approximate SPNs with continuous approaches.

The continuous Petri net (CPN) is an extension of the SPN aimed at finding an acceptable continuous approximation of the discrete behavior of the latter. The CPN has several advantages over its discrete counterpart, including the ability

✉ Hamid El-Moumen
elmoumen.hmd@gmail.com

Nabil El Akchioui
n.elakchioui@uae.ac.ma

[1] Faculty of Sciences and Techniques Al Hoceima, University Abdelmalek Essaadi, Tetouan, Morocco

to model continuous changes and time-dependent behaviors, and the ability to handle a large amount of information. To achieve this, several researchers have studied the fluidization of the SPN by the CPN (El Moumen et al., 2023a; Lefebvre et al., 2009; Recalde et al., 1999; Vazquez & Silva, 2009). Fluidization refers to the process of converting an SPN based on discrete events into a CPN based on deterministic continuous time (Recalde et al., 1999). The main goal of this conversion is to obtain a continuous behavior that approximates the behavior of systems modeled by SPNs, which will allow for a more accurate and exact analysis of these systems.

The process of fluidization involves adding continuous variables and differential equations to describe the evolution of the markings in each place of the SPN. This technique requires the use of control theory and numerical analysis to obtain performance calculations such as steady-state behavior of average markings and fast response time. However, fluidization can be challenging as it necessitates defining a continuous representation of the underlying system dynamics while preserving the stochastic behavioral structural properties (El-Moumen et al., 2023; Vazquez & Silva, 2009). It also involves solving information loss problems during the fluidization process and ensuring the coherence of the resulting continuous model.

Fluidization of SPNs can result in unexpected outcomes where the structural and behavioral properties may not be identical ((Lefebvre et al., 2009; Recalde et al., 1999). For instance, a PN can be live as a discrete system but non-live after fluidization (Vazquez & Silva, 2015), and a discretized bounded system can become non-boundary after fluidization (El Moumen et al., 2023a). The average throughput of the CPN may not always be an upper bound on that of the SPN (El Moumen et al., 2023a). While some methods exist for finding steady-state majors for CPN and SPN by solving linear programming problems (Giua & Silva, 2018); (David, 1993), no direct comparison exists between the two obtained majors (discrete and continuous). Additionally, the equilibrium points of SPN cannot be approximated directly by those of CPN. Standard fluidization under the semantics of infinite servers does not always lead to the same behavior (El Moumen et al., 2023a). The average markings and asymptotic average throughputs of SPN and CPN with similar structure and initial marking may not be identical in the general case (Akchioui, 2018). Researchers (El Akchioui, 2017; Lefebvre et al., 2009) have developed numerical approaches to obtain comparable behaviors between different models in this context. The first approach called "adaptive" (El & Choukrad, 2016; El Akchioui, 2017), and the second, "piecewise linear", were developed by (Akchioui, 2018; Lefebvre & Leclercq, 2012). The piecewise linear approach is described in the literature as a numerical method for approximating solutions to ordinary differential equations using piecewise linear functions over adaptively chosen time intervals. We added sufficient conditions, such as subdividing the marking trajectory into multiple intermediate phases, to ensure that the continuous fluid model converges to that of the stochastic model. The adaptive approach is also a numerical method for approximating solutions to ordinary differential equations, but it uses a strategy based on minimizing errors due to variations in markings and average throughputs. We also added conditions to ensure monotonic convergence. These two approaches solve the problem of the difference between asymptotic average markings and throughputs between stochastic and CPN. Finally, a more concise comparison and discussion of the results will be established and analyzed using simulations. The adaptive approach shows better convergence toward the steady state of stochastic models compared to the other approach.

The document is organized into four sections. Section 2 presents basic definitions of Petri nets (PNs), SPN and CPN. Section 3 discusses the limitations of using SPN and standard fluidization in a single region and multiple regions, with examples from the literature presented as a case study to illustrate these problems through numerical simulations. Section 4 describes two fluidization approaches: the piecewise linear and adaptive approaches. The same example is studied for the application of these two approaches, to compare them, discuss the results, and provide perspectives for future work.

2 Background

2.1 Petri nets (PNs)

A PN is a robust mathematical model used to represent a variety of systems operating on discrete variables. Its applications include the analysis, design, and reliability assessment of distributed systems, communication protocols, and other complex systems (Arzola et al., 2020; Rozenberg & Engelfriet, 1998). The original PN model did not incorporate the concept of time, which consists of places, arcs, transitions, and tokens, providing a foundation for modeling various properties of systems (David & Alla, 1994; Desel & Juhás, 2001; Murata, 1989).

In a formal context, a PN is defined by a quintuple $= (P, T, W, A, M)$, where (Desel & Juhás, 2001; Esparza, 1998):

- $P = \{P_i\}$, $i = 1, \ldots, n$, constitutes a finite set of n places, typically depicted as circles.
- $T = \{T_j\}, j = 1, \ldots, q$, represents a finite set of q transitions, often depicted as lines.
- $W \subseteq (P \times T) \cup (T \times P)$, signifies a set of arcs connecting places and transitions. The incidence matrix $W = (W^{PO} - W^{PR}) \in (Z)^{n \times q}$, with $W^{PR} = (w_{ij}{}^{PR}) \in (IN)^{n \times q}$ containing

values of arcs directed from P_i *to* T_j, and $W^{PO} = (w_{ij}{}^{po}) \in (IN)^{n\times q}$ containing values of arcs directed from T_j to P_i.
- *A:* $W \rightarrow \{1, 2, 3, \ldots\}$, signifies the weight associated with arcs in W.
- *M:* $P \rightarrow \{0, 1, 2, \ldots\}$, represents the marking, indicating the number of tokens, often depicted as dots or positive integers, in each place in P_i.

Timed PNs are a significant extension of conventional PNs designed to incorporate temporal variables into discrete event dynamic systems. They encompass the network's topological structure, labeling elements with temporal values, and establishing triggering rules based on time. Various approaches have been developed to model these timed dependencies, including deterministic timed transition PNs (Ramchandani, 1974), timed PNs by (Merlin, 1974), which define minimum and maximal wait times for transitions, deterministic timed place PNs (Coolahan & Roussopoulos, 1983), and deterministic timed arcs PNs (Zhu & Denton, 1988). Among these approaches, deterministic timed transition PNs, which associate time labels with transitions, stand out for their ability to link timing directly with transitions, providing flexibility for precise control over transition firing times. They are particularly suitable for evaluating system performance, especially in scenarios where time management is critical (Marsan, 1990; Seatzu, 2005).

A transition T_j is considered enabled when the current marking satisfies the enabling conditions. When enabled, a transition can fire, leading to the transfer of tokens from input places to output places based on the arc multiplicities. The sequencing of transitions becomes crucial when multiple transitions are enabled simultaneously. Determining the firing order is essential in such cases, while others may be delayed. The evolution of a PN is depicted through the marking graph, also recognized as the accessibility graph. Each node within this graph symbolizes a marking, and arcs illustrate potential transitions between markings, with transition labels indicating changes in marking. Place markings are denoted as $M(P_i)$ or simply m_i. The initial marking is represented as M_I, and the marking at time t is defined by $M(t)$. $E_j(M(t))$, signifies the enabled degree of transition T_j, determined for marking $M(t)$ according to (Júlvez et al., 2005; Lefebvre et al., 2010):

$$E_j(M(t)) = \min\left(M(P_i)/w_{ij}^{PR}\right), \text{ for all } P_i \in {}^{\circ}T_j. \qquad (1)$$

where ${}^{\circ}T_j$ represents the set of places upstream of T_j. For any $P_k \in {}^{\circ}T_j$, P_i is a critical place at t (time) for T_j with $i = \arg(min\ (m_k(t)/w_{kj}{}^{PR}))$ (Moumen et al., 2022).

Let $Y = \{y_{iP}\}$, $iP = 1\ldots, K_1$, denote the set of P-semi-flows, and $Z = \{z_{iT}\}$, $iT = 1\ldots, K_{-2}$, denote the set of T-semi-flows. A P-semi-flow $y \in (Z^+)^n$, satisfying the relation $y^T.W = 0$, corresponds to a marking invariant: $y^T.M = Y^T.M_I = C$, where C is a constant vector. This relation signifies the conservation of the weighted quantity of markings. A PN that accommodates one or more P-semi-flows in which all places occur at least once is termed conservative. Conversely, a T-semi-flow $z \in (Z^+)^q$, satisfying the relation $W.\ z = 0$, defines a potential cycle involving repetitive transitions while maintaining the marking invariant. A PN that admits one or more T-semi-flows in which all transitions occur at least once is referred to as consistent (Lefebvre & Leclercq, 2012).

2.2 Stochastic Petri Nets (SPNs)

The original PN model did not include the concept of time, leading to limitations in analyzing system performance and reliability. As a result, the notion of event duration associated with PN transitions needed to be introduced. Timed PNs provide the capability to not only depict a logical sequencing of occurrences but also account for their temporal aspects. They are useful for modeling systems where activations synchronize with external events and where system dynamics are influenced by temporal factors (David & Alla, 1994). To address this need, two main approaches were pursued. The first approach, timed PN, models event durations deterministically or within defined intervals. The second approach, SPN, represents event durations as random variables (Heiner et al., 2009; Karamanolis, 1999). Incorporating temporal information into transitions, timed PNs result in a more comprehensive representation. A specific case of timed PNs is SPN, where the firing times of transitions are considered random variables. More specifically, a particular case of SPN involves exponential distributions for firing times (Ajmone Marsan & Chiola, 1987; Haas & Shedler, 1989), with a parameter varying according to (round$(E_j(M)) \times \mu_j$), where $E_j(M)$ represents the enabling degree of transition T_j for a given marking M, and the function "round(.)" denotes the integer part of a number. The concept of SPN models was independently proposed by (Natkin, 1980; Molloy, 1981) in their respective doctoral dissertations. These models aimed to integrate formal description, correctness verification, and performance evaluation in the field of applied stochastic modeling (Marsan, 1990). The foundational idea of associating exponentially distributed random delays with PN transitions, crucial to SPNs, was prefigured by (Symons, 1980) in his work on Numerical PNs, offering a historical perspective on the evolution of these models.

An SPN, denoted as $< PN, \mu >$, associates the underlying PN with a firing rate vector $\mu = (\mu_j) \in (R^+)^q$. Each transition T_j in the SPN is characterized by a firing rate μ_j, representing the likelihood of T_j firing within a small-time interval dt, given that it has been activated with degree 1 at time t. The marking process of SPN is described using various elements, including the PN incidence matrix, the initial marking, the

firing rates, the firing policy, the server policy, and the execution policy (Lefebvre et al., 2009; Silva & Recalde, 2002). These characteristics are all utilized to describe the marking process of an SPN. The vector of the average throughput and average marking of an SPN depending on time, are named, respectively, $X_s(t)$ and $M_s(t)$. SPNs in this work have satisfied the hypotheses (A_1–A_5) (El Moumen et al., 2023a; Júlvez et al., 2005):

- (A_1) The labeled SPNs are limited by the bounds.
- (A_2) The labeled SPNs can be reset.
- (A_3) The firing policy follows a race policy, where the transition with the shortest firing time is considered to be the one that will fire next.
- (A_4) The server policy is infinite, meaning that each transition T_j has a minimal period (dm) determined by a stochastic length characterized by an exponential distribution with a parameter that varies according to (round$(E_j(M)) \times \mu_j$). This policy is characterized by the influence of the enabling degree.
- (A_5) The execution policy is of the form of "resampling memory," where at the start of labeling, all transitions that were previously enabled have their remaining firing time reset.

These assumptions collectively provide a solid foundation for effectively modeling and analyzing SPN behavior, specifically concerning how markings evolve and the precise timing of transition firings. When focusing on the average marking and average throughput of SPNs, SPNs are configured to encompass an accessibility graph denoted as $A(SPN, M_1)$ with finite states. This graph's labeling process aligns seamlessly with a Markov model that exhibits an isomorphism to $A(SPN, M_1)$. Consequently, this configuration allows us to calculate the asymptotic behavior of the SPN based on the probability of reaching the steady state within the Markov model (El-Moumen et al., 2023; Moumen et al., 2022).

In the context of operational SPNs adhering to the aforementioned assumptions and operating within a finite state space, the SPN presents a marking graph that is isomorphic to the state space of a Markov model. Within this framework, determining the SPN's steady state becomes feasible by evaluating the probabilities associated with the Markov model states. The vector of steady-state probabilities is defined by the solution of (El & Choukrad, 2016):

$$\Pi_S \cdot A(\mu) = 0 \text{ and } \Pi_S \cdot 1_N = 1. \tag{2}$$

with $\Pi_S = (\pi_{Sk})^{1 \times N}$, the vector of steady-state probabilities of the Markov model related to N states. $A(\mu)$, as the Markov model generator associated with the SPN, is a square matrix of dimension $N \times N$,N being the finite number of states of the linked Markov model and $1_N = (1,\ldots,1)^T$ represents a vector of dimension N whose all components are equal to 1.

Let $X_s = (x_{sj} \in (R^+)^q)$ represent the average throughput vector of SPN and $M_S = (m_{Si}) \in (R^+)^n$ represent the average markings vector of SPN. As a consequence, from the vector Π_S, we will deduce the average throughputs of transitions as well as the average markings of places as (Lefebvre et al., 2010):

$$x_{sj} = \mu_j \cdot \sum_{k=1}^{N} \left(E_j(M_k) \cdot \pi_k\right). \tag{3}$$

$$m_{si} = \sum_{k=1}^{N} m_{ki} \cdot \pi_k. \tag{4}$$

where $M_K = (m_{ki}) \in (R^+)^n$ signifies the vector of marking matching the state k of the Markov model. When it comes to the ergodic Markov Model, this method gives an analytical solution of the steady state of the SPN, but it necessitates computing the transition matrix $A(\mu)$ (Lefebvre et al., 2009; Vazquez & Silva, 2015), as a result, the SPNs accessibility graph $A(SPN, M_1)$ is isomorphic to the Markov model (Vázquez et al., 2008). N rises exponentially. For large-scale systems, the calculation time and storage needs to evaluate $A(SPN, M_1)$ become more relevant. In this case, for the Markov model, SPN can be thought of as a stochastic estimator. The benefit of this estimator is that it eliminates the need to determine $A(SPN, M_1)$, but, the stochastic estimator is slow to converge, especially for rare events.

In the realm of SPNs, analysis involves the exploration of two distinct yet mutually reinforcing aspects. The first aspect delves into the preservation properties within a PN, derived from P-semi flows and T-semi flows, providing valuable insights into system behavior. The second aspect focuses on the analysis of a continuous-time, discrete-state space Markov process, commonly recognized as a bounded PN (Marsan, 1990; Silva & Recalde, 2002). These two complementary methods together enable a comprehensive exploration of system dynamics within the domain of SPNs. This framework not only facilitates the simulation of complex systems but also offers a practical alternative to state graph-based Markov analysis, especially for large systems where the combinatorial explosion can render traditional methods impractical (Kuntz et al., 2021). Furthermore, SPNs serve as estimators of Markov models, assisting in the comparison and evaluation of system performance indicators.

To facilitate the determination of system performance indicators and the comparison of the random behavior of the SPN with that of a homogeneous Markov model with a finite state space, the algorithm of the stochastic estimator is depicted in Fig. 1 (El Moumen et al., 2023a).

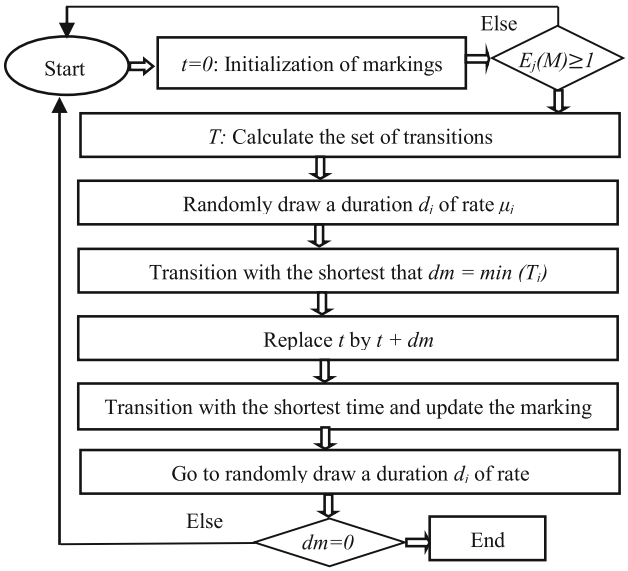

Fig. 1 Steady state by SPNs algorithm

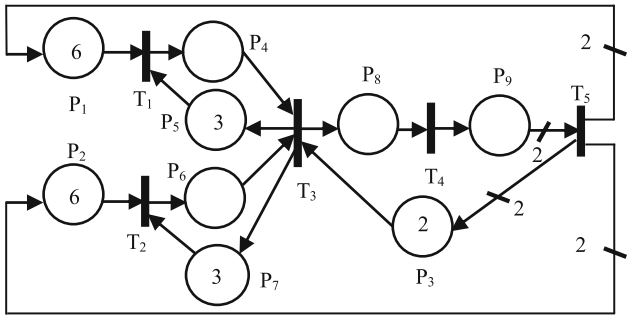

Fig. 2 Manufacturing system

The equation governing the instantaneous velocity of the transition T_j is given by (Lefebvre & Leclercq, 2012):

$$x_{cj} = x_{\max j} \cdot E_j(M_c(t)). \tag{6}$$

2.3 Timed Continuous Petri Nets (CPNs)

Timed continuous Petri nets (TCPNs) represent an extension of PN designed for modeling and analyzing dynamic systems that evolve over time. They are utilized to capture systems that exhibit both temporal and continuous characteristics, making them particularly well-suited for modeling reactive systems in fields such as industrial automation, communication, and robotics (El Moumen et al., 2023a). TCPNs combine the features of PNs, timed systems, and continuous systems to accurately depict the dynamic behavior of systems (Silva & Recalde, 2002). While TCPNs are commonly denoted as CPNs, they have been deliberately developed to provide continuous approximations of the discrete behaviors of PNs. CPNs are distinguished by their consistent maximal firing speeds and employ an infinite server semantic to facilitate a seamless transition between discrete and continuous modeling paradigms. The marking of each place is represented as a continuous, non-negative real-valued function of time, as described by (Lefebvre et al., 2010; Seatzu, 2005; Silva & Recalde, 2004). A CPN is formally defined as $< PNs, X_{\max} >$, where $X_{\max} = \text{diag}(x_{\max j}) \in (R^+)^{q \times q}$ is the diagonal matrix of the maximal firing speeds $x_{\max j}$, with $j = 1,..,q$.

Let $M_c(t) = (m_{ci}) \in (R^+)^n$ be the vector representing the continuous markings $m_{ci}(t)$ of place P_i, with $i = 1,..,n$. Likewise, let $X_c(t) = (x_{cj}) \in (R^+)^q$ be the vector representing the continuous throughputs of transition T_j. The evolution of the marking in CPN can be described by (Lefebvre et al., 2010):

$$dM_c / dt = W \cdot X_C(t),\ M_c(0) = M_I. \tag{5}$$

3 SPNs and CPNs: Problem Statements

3.1 Complexity of the Reachability Graph for SPN

As an example, we will consider the example modeled by (Júlvez et al., 2005) presented in Fig. 2. This PN is used to model a manufacturing system with *5* machineries (T_1–T_5), and *3* resources limited tools (P_1–P_3). In this PN model, the vector of the parameters of the transitions μ and the initial marking M_1, are given by, $\mu = (1,1,1,1,1)^T$, $M_1 = k(6, 6, 2, 0, 3, 0, 3, 0, 0)^T$ where $k \in IN$.

Table 1 shows the variation in the number of states N and the computation time required to calculate the reachability graph, based on the parameter k (Silva & Recalde, 2002). We consider two cases: the first has $M(P_3) = 2$, and the second has $M(P_3) = 4$. These cases clearly illustrate the complexity associated with the reachability graph.

Table 1 indicates that as the parameter k increases, particularly when the marking of place P_3 increases, the number of states in the marking graph increases exponentially (Akchioui, 2018; Murata, 1989). Although the SPN does not need to compute the marking graph, the increase in the number of states leads to a longer computation time.

Consider the SPN described in Fig. 3 (Lefebvre & Leclercq, 2012) that contains two joint synchronizations in T_1 and T_2 with initial marking $M_1 = (5, 0, 0, 0, 4)^T$ and firing rate μ with $\mu = (3\ 1\ 1\ 10)^T$. This PN has a single firing invariant defined by the T-semi flow $z_1 = (1\ 1\ 1\ 1)^T$ and two marking invariants defined by the P-semi flows $y_1 = (0\ 0\ 0\ 1\ 1)^T$, and $y_2 = (1\ 1\ 2\ 1\ 0)^T$.

Figure 4 illustrates the evolution of the estimated marking of place P_1 in blue and the average marking in red, as obtained

Table 1 Number of states and calculation time of the reachability graph in function of k

k	Number of states (N)		Calculation time (s)	
	$m(P_3) = 2$	$m(P_3) = 4$	$m(P_3) = 2$	$m(P_3) = 4$
1	96	205	0.084	0.113
2	735	1885	2.141	8.304
3	2800	7796	20.104	164.665
4	7605	22187	150.462	1321.804
5	16826	50801	1018.708	6959.009

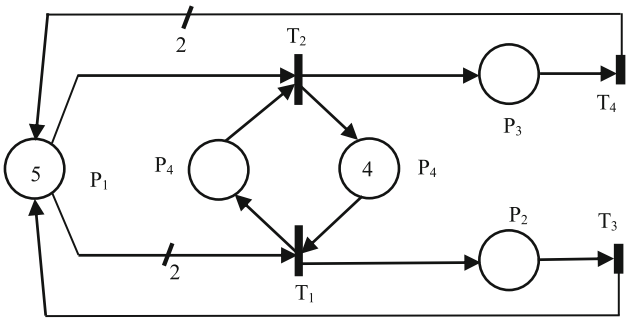

Fig. 3 Non-ordinary SPN with two joins and $M_1 = (5\ 0\ 0\ 0\ 4)^T$

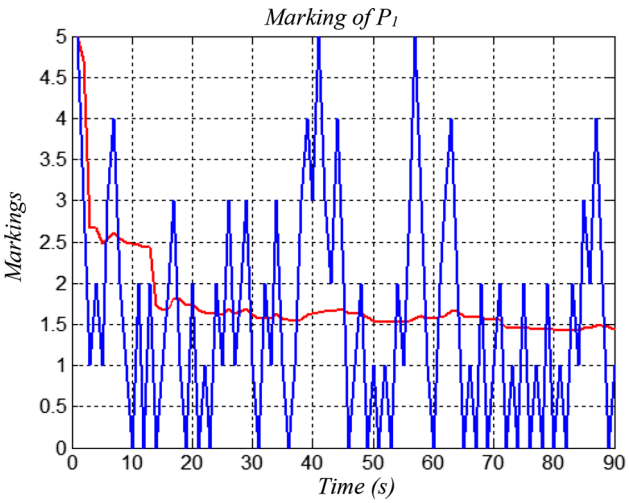

Fig. 4 Markings evolution $M_{s1}(t)$ of *SPN* in function of time for example of Fig. 3

by the SPN simulator using the firing rate $\mu = (3\ 1\ 1\ 10)^T$ shown in Fig. 3.

Simulation using SPNs leads to longer calculation times to reach a steady-state behavior, especially when the initial marking generates a large number of states. Therefore, we can explore a solution to expedite this calculation time by employing CPN simulation to estimate the evolution of average markings and throughputs. Unfortunately, SPNs and CPNs exhibit different asymptotic behaviors.

3.2 Standard Approximation of SPNs

The standard approximation of SPNs by CPNs involves replacing the input and output arcs of each place with continuous arcs to model uncertain dynamic systems using differential equations (Júlvez et al., 2005; Vázquez et al., 2008). However, this approach often results in structural and behavioral differences between the two models (Benaya et al., 2018; Silva & Recalde, 2004). For example, a PN can be live as a discrete model but non-live after fluidization (Lefebvre & Leclercq, 2012; Navarro-Gutiérrez et al., 2022), and a discretized bounded system can become non-bounded after fluidization (Horton et al., n.d.). The average throughput of the CPN is not always an upper bound on that of the SPN (Recalde et al., 1999). While there are methods for finding steady-state majors for both CPN and SPN, obtained through solving linear programming problems (Lefebvre et al., 2009; Seatzu, 2005; Vazquez & Silva, 2009), there is no direct comparison between the two majors, discrete and continuous. Additionally, equilibrium points of the SPN cannot be directly approximated by those of the CPN due to differences in behavior resulting from standard fluidization approaches. As a result, the average markings and asymptotic average throughput of SPN and CPN with similar structures and initial markings may not be identical in general. To interpret this issue, we will provide a concrete example and ensure that we are in the same context as the problem. Then, we will establish a proof base to reach the actual solution. This approach will enable us to gain a better understanding of the situation and propose an effective solution to resolve the issue, which involves finding a direct convergence solution between the two models.

Consider the example presented in Fig. 3. Table 2 presents the results of the standard approximation under the infinite server semantics.

Figure 5 shows the simulation of SPN of Fig. 3 with standard approximation ($x_{\max j} = \mu_j$), we only consider the marking of the places P_1, P_4 and P_5.

Figure 5 displays the evolution of markings by SPN and CPN from Fig. 3, enabling a comparison between the two models. In this context, CPN simulation is conducted under

Table 2 Markings and throughputs of stochastic and continuous behaviors in Fig. 3

$\mu = (3, 1, 1, 10)^T$	m_1	m_2	m_3	m_4	m_5	$x_{1,..,4}$
SPN	1	0.8	0.1	3	1	0.80
CPN	0.5	0.5	0.1	3.8	0.2	0.54

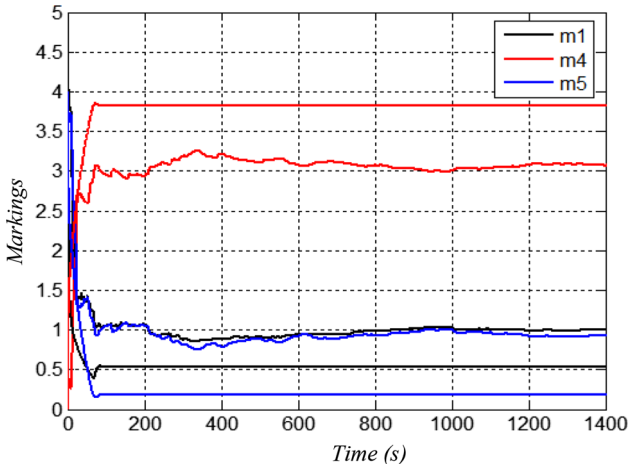

Fig. 5 Markings evolution $M_c(t)$ and $M_s(t)$ of CPN and SPN in function of time for example of Fig. 3

the infinite server semantics with $x_{\max j} = \mu_j$. Figure 5 clearly illustrates that the behaviors of continuous and stochastic average markings are distinct. This discrepancy arises due to the presence of weighted arcs and synchronization, leading to the emergence of multiple distinct regions, as indicated by the "min(..)" function in the activation degree expression. It is worth noting that the standard approximation method does not guarantee identical behavior between SPNs and CPNs (Silva & Recalde, 2004).

3.3 Region in the Reachability Graph for CPN

In this section, we delve deeper into the concept of regions, which play a pivotal role in our analyses. The notion of the region appears because of the "min(..)" function in the activation degree expression (El Akchioui, 2017; Lefebvre et al., 2010). These regions are vital for understanding the behavior of our model and its various configurations. The marking area is separated into k regions L_K (Akchioui, 2018) (some regions may remain empty). Each L_K region is defined by its unique combination or configuration (El Moumen et al., 2023a), which is also referred to as the *PT*-sum$(L_K) = \{(P_i, T_j)\}$. The *PT*-sum for a given L_K can be expressed as $\{(P_i, T_j)\}$, where P_i represents the critical place of T_j within L_K (Silva & Recalde, 2002). The number of configurations is closely tied to the number of synchronizations and the count of places leading to synchronization transitions, denoted as $K = |{}^\circ T_1| \, x \ldots x \, |{}^\circ T_q|$. The *PT-sum* (L_k), is formally defined as the sum of all combinations (P_i, T_j), specified below:

$$PT - \text{sum}(L_K) = \Big[\big(P_i, T_j\big)s \cdot m \cdot \forall M_c(t) \in L_K, x_{cj}(t) = x_{\max j}(t) \cdot m_{ci}(t) \Big/ w_{ij}^{PR}\Big]. \quad (7)$$

Each L_K region is uniquely characterized by a matrix constraint $L_k = (l_{ij}{}^k) \in (R^+)^{qxn}$, where $i = 1,..., q$, $k = 1,...,K$ and $j = 1,..., n$. The constraints within L_k are as follows:

- for all $T_j \in T$, $l_{ji}{}^k(k,j) = 1/w_{i(k,j)j}{}^{PR}$,
- Otherwise, $l_{ji}{}^k = 0$.

Consequently, within each L_K, we can represent the maximal firing speeds vector as $X_c(t) = X_{max}.\ L_K.\ M_c(t)$, as follows:

$$dM_c(t) \big/ dt = W \cdot X_{\max} \cdot L_K \cdot M_c(t), \ \forall M_c(t) \in L_K. \quad (8)$$

Consider the PN illustrated in Fig. 3, which is a non-ordinary PN that contains two joint synchronizations in T_1 and T_2 with $\mu = (3, 1, 1, 10)^T$ and $M_1 = (5\ 0\ 0\ 0\ 4)^T$. The existence of synchronizations leads to the presence of multiple distinct regions, with the number of regions dependent on the number of synchronizations in the PN. The CPN in Fig. 3 contains two synchronizations, reflected in the choice of maximal firing speed corresponding to the validation degree expression. The maximal firing speeds are determined as follows:

$$\begin{cases} X_{c1}(t) = x_{\max 1} \cdot \min\big(m_{c1}(t) \big/ 2, m_{c5}(t)\big) \\ X_{c2}(t) = x_{\max 2} \cdot \min(m_{c1}(t), m_{c4}(t)) \\ X_{c3}(t) = x_{\max 3} \cdot m_{c2}(t) \\ X_{c4}(t) = x_{\max 4} \cdot m_{c3}(t) \end{cases}. \quad (9)$$

The existence of the "*min*" operator in the calculation of $x_{c1}(t)$ and $x_{c2}(t)$, leads to the existence of four regions L_1 to L_4. Each region is linked to a *PT-sum*(L_K) (Silva & Recalde, 2002), $k = 1,..,4$. Table 3 summarizes the results obtained from each region L_K.

Note that P_1 is a critical place for both transitions T_1 and T_2; therefore, L_1 is a critical region. The speeds of the two transitions (T_1, T_2), depend on the same place P_1. The following constraint matrix serves as indicators for the regions L_1 toL_4**:**

Table 3 Regions and configurations for the CPN in Fig. 3

Regions	Configurations
L_1	$\{(P_1, T_1), (P_1, T_2), (P_2, T_3), (P_3, T_4)\}$
L_2	$\{(P_1, T_1), (P_4, T_2), (P_2, T_3), (P_3, T_4)\}$
L_3	$\{(P_5, T_1), (P_1, T_2), (P_2, T_3), (P_3, T_4)\}$
L_4	$\{(P_5, T_1), (P_4, T_2), (P_2, T_3), (P_3, T_4)\}$

$$L_1 = \begin{bmatrix} 1/2 & 0 & 0 & 0 & 0 \\ 1 & 0 & 0 & 0 & 0 \\ 0 & 1 & 0 & 0 & 0 \\ 0 & 0 & 1 & 0 & 0 \end{bmatrix} \quad L_3 = \begin{bmatrix} 0 & 0 & 0 & 0 & 1 \\ 1 & 0 & 0 & 0 & 0 \\ 0 & 1 & 0 & 0 & 0 \\ 0 & 0 & 1 & 0 & 0 \end{bmatrix}$$

$$L_2 = \begin{bmatrix} 1/2 & 0 & 0 & 0 & 0 \\ 0 & 0 & 0 & 1 & 0 \\ 0 & 1 & 0 & 0 & 0 \\ 0 & 0 & 1 & 0 & 0 \end{bmatrix} \quad L_4 = \begin{bmatrix} 0 & 0 & 0 & 0 & 1 \\ 0 & 0 & 0 & 1 & 0 \\ 0 & 1 & 0 & 0 & 0 \\ 0 & 0 & 1 & 0 & 0 \end{bmatrix}$$

The region L_1 is a critical region reachable from the initial marking M_1. In the following, we subdivide CPN into different classes, depending on the nature of the synchronizations.

3.4 Approximation in Multiple Regions and in the Critical Region

Let us consider the example in Fig. 3, where five SPNs with different firing rates, namely SPN_1 through SPN_5, denoted as $\boldsymbol{\beta_1}$ to $\boldsymbol{\beta_5}$, are available. In this study, we have selected three SPNs from the critical regionL_1, namely $\boldsymbol{\beta_2}$, $\boldsymbol{\beta_3}$ and $\boldsymbol{\beta_5}$, to highlight the pivotal role played by this specific region in delineating the distinctions between SPNs and CPNs. The choice of these particular SPNs was made to focus our analysis on the region that exhibits unique characteristics and challenges within the context of our study. This selection allows us to explore and better understand the influence of the critical region on the differences between SPNs and CPNs.

Table 4 gathers the results of the standard approximation of SPNs in Fig. 3 in different firing rates under the infinite server semantics with the same structure and the same M_1.

Figures 6 and 7 show the projections in the $(m_1, m_2{+}2{\cdot}m_3)$ plane of the stochastic and continuous average markings, respectively, in different accessible regions as a function of five random draws of transition rates and maximal firing speeds.

The SPN and CPN regions are different. For example, in Fig. 6, β_2, β_3, and β_5 are located in region L_1, but after fluidization presented in Fig. 7, they move to regionL_3. This difference is due to the more sincere division into several regions due to the presence of the "min(..)" function in the definition of the degree of activation, resulting in the

Table 4 Stochastic and continuous markings and throughputs of the SPN and CPN in Fig. 3 for different values of $X_{\max j} = \mu_j$

$SPN_{1\ldots4}$	μ	M_s	X_s
β_1	$(3\ 3\ 8\ 9)^T$	$(2.4\ 0.3\ 0.3\ 1.6\ 2.4)^T$	2.82
β_2	$(6\ 2\ 3\ 0.5)^T$	$(0.6\ 0.2\ 1.3\ 1.6\ 2.4)^T$	0.64
β_3	$(3\ 1\ 1\ 10)^T$	$(1\ 0.8\ 0.1\ 3\ 1)^T$	0.80
β_4	$(7\ 0.5\ 2\ 3)^T$	$(0.8\ 0.2\ 0.1\ 3.7\ 0.3)^T$	0.39
β_5	$(1, 3, 1, 3)^T$	$(1.03\ 0.8\ 0.8\ 3.01\ 0.98)^T$	0.80
$CPN_{1\ldots4}$	$X_{\max} = \text{diag}(\mu)$	M_c	X_c
β_1	diag (3 3 8 9)	$(2.5\ 0.5\ 0.4\ 1.2\ 2.8)^T$	3.71
β_2	diag(6 2 3 0.5)	$(0.1\ 0.1\ 0.4\ 3.9\ 0.1)^T$	0.21
β_3	diag (3 1 1 10)	$(0.5\ 0.5\ 0.1\ 3.8\ 0.2)^T$	0.54
β_4	diag (7 0.5 2 3)	$(0.7\ 0.2\ 0.1\ 3.9\ 0.1)^T$	0.3
β_5	diag (1, 3, 1, 3)	$(0.53\ 0.53\ 0.05\ 3.82\ 0.17)^T$	0.53

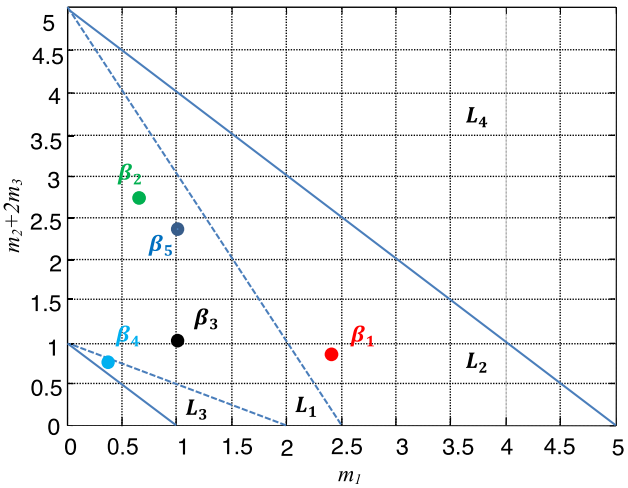

Fig. 6 Marking $M_s(t)$ for different firing rates of the SPN for example of Fig. 3

CPNs behavior being piecewise linear (Lefebvre & Leclercq, 2012). Note that in Fig. 6, SPN β_1 and β_4 are located outside of the critical region L_1. According to fluidization, in Fig. 7 they remain in the same region as the SPNs. However, other SPNs such as β_2, β_3, and β_5 do not remain in the same region as the SPNs. This shows that the critical region plays an important role in this difference. These results show that the standard approximation of SPNs by CPNs with multiple regions and particularly the critical region does not lead to the same behavior of the asymptotic average marking and that the behavior of SPNs is not always accurately approximated by CPNs.

To overcome this problem, two numerical approaches of fluidization have been studied in (El Moumen et al., 2023a;

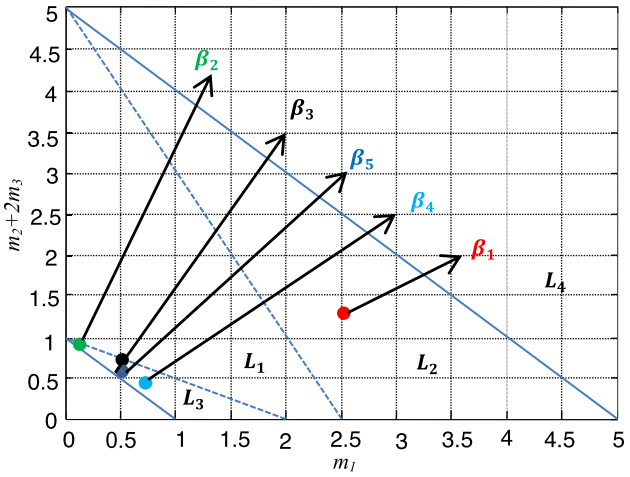

Fig. 7 Marking $M_c(t)$ for different maximal firing speeds of the CPN for example of Fig. 3

Júlvez et al., 2005; Lefebvre & Leclercq, 2012; Lefebvre et al., 2009) to obtain a CPN whose average behavior in steady state is equivalent to the average behavior of a given SPN, under the semantics of the infinite server. We will apply these approaches to the previous example, Fig. 3, to compare and discuss them.

4 Numerical Approaches to Fluidization and Comparison

Fluidization is an interesting alternative for estimating the asymptotic behavior of stochastic processes using CPNs. The synchronization is a key element of this approximation. Specifically, the presence of multiple regions, and particularly the existence of critical regions, complicates the standard approximation of the SPNs. In this section, we investigate two different approximation approaches: the piecewise linear approach (Lefebvre & Leclercq, 2012) and the adaptive approach (El Akchioui, 2017; El Moumen et al., 2023a). The piecewise linear approach is described in the literature as a numerical method for approximating solutions to ordinary differential equations using piecewise linear functions over adaptively chosen time intervals. We have shown that fluidization is not guaranteed when the initial marking exists in the critical region, and therefore we have added sufficient conditions, such as subdividing the marking trajectory into multiple intermediate phases, to ensure convergence in all regions, especially in the critical region. The adaptive approach is also a numerical method that compensates for errors due to variations in marking and throughput rates and necessary conditions will be added to ensure monotone convergence. Both of these approaches solve the problem of the difference between asymptotic markings and throughputs between stochastic and CPN models. Finally, a more concise comparison and discussion of results will be established and analyzed using simulations.

The first one is characterized by maximal firing speeds of transitions defined and different in each region, allowing us to define a new piecewise linear CPN. The second one is characterized by maximal firing speeds of transitions modified by a nonlinear adaptive law, based on minimizing errors due to variations of marking and average firing throughput. Finally, we will apply these approaches to the previous example shown in Fig. 3. We will choose the case of SPN β_3, from the critical region L_1 as our case for comparison and discussion of these two approaches is grounded in its significance within the context of the study. This choice allows us to effectively illustrate the implications and outcomes of applying these two distinct approaches in a region known for its critical characteristics.

4.1 Piecewise Linear Approach (CPN-PW)

The piecewise linear approach is a modeling tool that divides the approximation of markings into several phases, making it suitable for systems with multiple phases. The maximal firing speed is defined as a piecewise continuous function, allowing the CPN to converge to the stochastic marking. Sufficient conditions are established for the fluid model to converge to the stochastic average marking in both the single region and multiple region cases. Convergence is guaranteed for the single region, but for the multiple region case, particularly the critical region, sufficient conditions are established. This results in the definition of a new piecewise linear CPN (Lefebvre & Leclercq, 2012), where the marking evolves in each region and has different maximal firing speeds of transitions from other regions.

Definition 1 Equivalent average marking.

Let us consider a CPN. Let M_c be the vector of markings and X_c the vector of stationary state speeds. X_c verifies:

$$W \cdot X_c = 0 \quad \text{with } X_c > 0. \tag{10}$$

In the L_K region, (8) can be rewritten, aiding in the characterization of the stationary state of the CPN as:

$$W \cdot X_{\max} \cdot L_k \cdot M_c = 0. \tag{11}$$

The system of equations obtained from (11) is however insufficient to determine $X_{\max}$. When considering the marking invariants, we derive the compatible system as:

$$\underbrace{\begin{pmatrix} W \cdot X_{\max} \cdot L_k \\ Y^T \end{pmatrix}}_{S(X_{\max})} \cdot M_c = \underbrace{\begin{pmatrix} 0 \\ Y^T \cdot M_I \end{pmatrix}}_{C}. \tag{12}$$

In the case where the determination of the steady-state marking has a unique non-negative solution, the expression of the marking as a function of $X_{\max}$ can be obtained as:

$$M_c = f(X_{\max}). \tag{13}$$

The function f depends on the maximal firing speeds and can be obtained by the resolution of the (12) provided that the matrix $(L_K{}^T.\ X_{max}.\ W^T|Y)^T$ is of full rank in columns (i.e., of rank$n$). In this scenario, the maximal speed matrix can be determined, and the average throughputs can be calculated as follows:

$$X_{\max} \cdot L_k \cdot M_c = X_c. \tag{14}$$

Definition 2 Global asymptotic equivalence.

Consider as $SPN < M_I, \mu, M_s >$ with $M_I \in L_k$ and a CPN with the same structure, the same M_I and different maximal firing speeds of SPN firing rates. In each L_k, $M_c(t)$ satisfy (8). Consequently, when the marking trajectory remains in the M_I region it tends to M_c that satisfies (8). As long as $\text{rank}(S(X_{\max})) = rank(S(X_{\max}).\ C) = q$, the system of (12) becomes invertible, whose solution allows determining the continuous average marking which verifies (15). As long as M_c converges to M_s satisfy $M_c = M_s$, the solution of (12) also allows computing $Mc = f(X_{\max})$. The long-term exact solution for M_c is as follows:

$$\begin{cases} M_c = (S^T(X_{\max}) \cdot S(X_{\max}))^{-1} \cdot S^T(X_{\max}) \\ M_s = (S^T(X_{\max}) \cdot S(X_{\max}))^{-1} \cdot S^T(X_{\max}) \cdot C \end{cases}. \tag{15}$$

When $M_c(t)$ and $X_c(t)$ converge to M_s and X_s, respectively, as t tends to infinity, and if $M_c(t)$ satisfies the condition, then the rank of $S(X_{\max}) = q$, and $X_{\max}$ satisfies (Lefebvre & Leclercq, 2012):

$$\begin{cases} X_s = X_{\max} \cdot L_k \cdot (S^T(X_{\max}) \cdot S(X_{\max}))^{-1} \cdot S^T(X_{max}) \cdot C \\ M_s = (S^T(X_{max}) \cdot S(X_{max}))^{-1} \cdot S^T(X_{max}) \cdot C \end{cases}. \tag{16}$$

In each L_K, $X_c(t)$ satisfies $X_c(t) = X_{\max}.\ L_K.\ M_c(t)$. In particular, if $M_s \in L_K$, X_s holds:

$$X_s = X_{\max} \cdot L_k \cdot M_s. \tag{17}$$

Definition 3 Piecewise Continuous Petri net (CPN-PW).

A *CPN-PW* is seen as a combination of several timed CPN: $\{CPN_k,\ k = 1,..,\ K\}$ with $CPN_k = \{P,\ T,\ W^{PO},\ W^{PR},\ X_{\max k}\}$ that evolves only in the region L_k. $X_{\max k}$, $k = 1,..,\ K$ represents the matrix of maximal firing speeds defined in each region (Lefebvre & Leclercq, 2012).

The CPN-PW behaves like a collection of several CPNs in a single CPN. The matrixes of maximal firing speeds $X_{\max k}$, $k = 1,...,K$ of a CPN-PW are calculated for each region L_k. Each CPN has different maximal firing speeds. The asymptotic average markings of a CPN-PW satisfy the form of (11) in each region L_k. We continue with the example in Fig. 3 to illustrate the global asymptotic equivalence in the $\boldsymbol{\beta_3}$ SPN that exists in the L_k critical region.

4.2 Adaptive Approach

The adaptive approach is aimed at adapting all maximal firing speeds of the CPNs through an adaptive controller. These speeds are considered time-varying functions and are updated to ensure the modified CPN converges to the SPN. It corrects errors in throughput and marking by referring to the asymptotic stochastic average throughput and average marking to be reached. Therefore, the adaptive maximal firing speeds for the nonlinear CPN (NL-CPN) are defined.

Definition 4 Nonlinear CPN.

A Nonlinear CPN: (NL-CPN) $= (P,\ T,\ W^{PR},\ W^{PO},\ M_s,\ X_s)$, is governed by the adaptation law of the maximal firing speeds. This law constitutes a system of $(n + q)$ differential equations under the constraint $X_{\max} \geq 0$, as proposed by (El Akchioui, 2017; Lefebvre et al., 2009):

$$\dot{X}_{\max} = \eta \cdot \text{diag}(\mu) \cdot \left(\left(W^T\right) \cdot (M_s - M_c(t)) + (X_s - X_c(t))\right). \tag{18}$$

where $\text{diag}(\mu)$ is the diagonal matrix SPN firing rates, η is the adaptation parameter, $(X_s{-}X_c(t))$ represents the error related to the continuous and stochastic average throughput, and the vector $(M_s{-}M_c(t))$ the error due to variations in the stochastic and continuous average markings.

To determine the variations of the maximal firing speed associated with the transition T_j, we considered the transition T_j and w_j which defines the column j of the W. The variations of the maximal firing speeds of transition T_j depend on the places $({}^\circ T_j)$ and downstream $(T_j{}^\circ)$ of the transition in consideration, in the following different cases:

- If at time t, all places$P_i \in {}^\circ T_j$, verify $m_{si}{-}m_{ci}(t) > 0$ and all places $P_k \in T_j{}^\circ$, verify $m_{sk}{-}m_{ck}(t) < 0$ then $w_j{}^T.(m_s{-}m_c(t)) < 0$, this leads to decrease the maximal firing speeds x_{maxj} of T_j.
- If at time t, all places $Pi \in {}^\circ T_j$, verify $m_{si}{-}m_{ci}(t) < 0$ and all places $P_k \in Tj^\circ$, verify $m_{sk}{-}m_{ck}(t) > 0$ then $w_j{}^T.(m_s{-}m_c(t)) > 0$, this leads to increase the speed x_{maxj} of T_j.

On the other hand, the direction of variation of the speed $X_{\max}$ also depends on the instantaneous firing speed associated with the transition T_j, in the following cases:

– If $x_{sj}-x_{cj}(t) < 0$, the maximal firing speeds $x_{\max j}$ of T_j decreases.
– If $x_{sj}-x_{cj}(t) > 0$, the maximal firing speeds $x_{\max j}$ of T_j increases.

But when these previously mentioned criteria are not satisfied concurrently, the convergence is no more monotonous. Finally, we will illustrate and compare these different approaches in an example.

4.3 Comparison and Discussion

In this sub-section, we will study the results of the two different fluidization approaches presented previously to illustrate and compare them.

In the first approach studied in this section, the CPN-PW converges to the stochastic average marking in a single region with no problem, and its continuous path remains in the same region as the initial marking. In this case, the steady state converges directly to the stochastic target points. However, when convergence occurs in multiple regions, a problem of converging this model toward the stochastic target points will arise. This problem is manifested by the existence of the critical region, which directly complicates the fluidization by this approach. In this case, we subdivide the marking trajectory into multiple phases and intermediate points to move from one region to another to achieve convergence in the critical region. Table 5 gives the modified continuous average behavior obtained from CPN-PW fluidization of SPN β_3 in Fig. 3.

Table 5 shows that fluidization CPN-PW is not achieved directly; for this purpose, the marking trajectory is divided into several phases and intermediate points M_{int} to move from one region to another, to achieve stochastic marking of β_3. The SPN β_3 and the initial marking M_{I} are in two different regions, to reach β_3 from M_1, two successive phases appear, first, to reach the common intersection of the two regions L_2 and L_1 whose $M_{\text{int}} = (2.1\ 0.3\ 0.3\ 1.\ 6\ 2.4)^T$, we applied the constant positive matrix velocity $X_{\max 1} = x_{\max 4}.\text{diag}(0.3\ 0.2\ 0.9\ 1)^T$, where $x_{\max 4}$ represents one degree of freedom, in the second stage we apply the velocity $X_{\max 2} = \text{diag}(3.6\ 1.8\ 5.1)^T$ to achieve the final value $\beta_3 = (1.03\ 0.80\ 0.08\ 3.01\ 0.98)^T$ (Fig. 8).

In the last approach studied in this section, we proposed to modify the definition of the parameters that characterize the maximal firing speeds of the transitions for the CPN, using multiplicative coefficients applied to the maximal firing speeds of all transitions. These coefficients are considered as time dependent functions according to the adaptive law (18). This law minimizes the errors due to variations in markings and throughputs over time in order to have a continuous steady state equivalent to that of the SPN. Table 6 gives the modified continuous average behavior obtained by adapting all the maximal firing speeds of the SPN β_3 in Fig. 3.

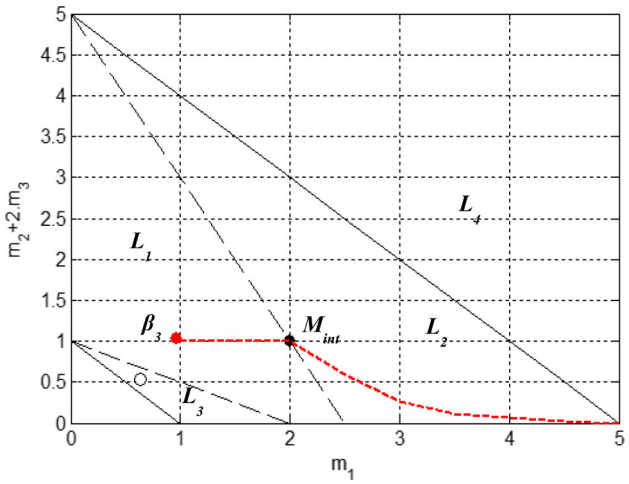

Fig. 8 Continuous piecewise approximation of the stochastic average marking of the SPN in Fig. 3

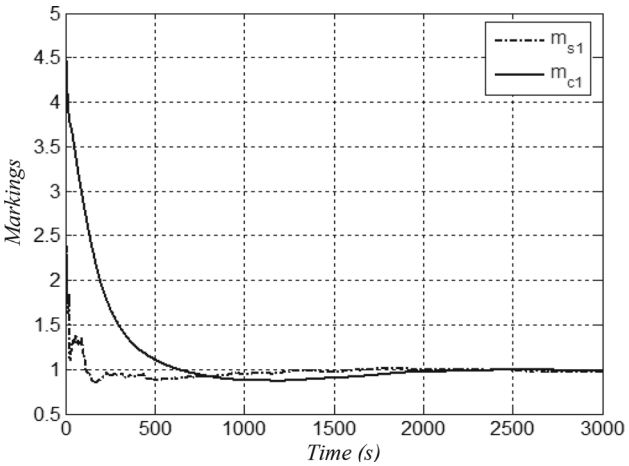

Fig. 9 Evolution of the continuous and stochastic markings of the place P_1 in function of time

Each maximal firing speed will be corrected by a multiplicative factor. Therefore, only the marking of place P_1 will be represented. Figure 9 shows the continuous average marking and the asymptotic stochastic average marking of the square P_1, after the modification of the maximal firing speeds of CPN in Fig. 3.

Minimizing the errors due to variations in markings and throughput allows for a new CPN whose average behavior is equivalent to that of the SPN. The implementation of this approach requires knowledge of the asymptotic stochastic behavior $\beta_3 = (1.03\ 0.8\ 0.08\ 3.01\ 0.98)^T$ that is desired to be achieved.

This approach is the most effective for approximating the throughput and average markings of the SPN using the CPN.

Table 5 Modified continuous behaviors after fluidization by CPN-PW in Fig. 3

	m_1	m_2	m_3	m_4	m_5	$x_{1,..,4}$
SPN	1.03	0.80	0.08	3.01	0.98	0.80
CPN	1.08	0.864	0.108	2.88	1.08	0.85
Relative error	0.05	0.064	0.028	0.13	0.1	0.05

Table 6 Modified continuous behaviors after adaptation of all maximal firing speeds of CPN in Fig. 3

	m_1	m_2	m_3	m_4	m_5	$x_{1,2,3,4}$
SPN	1.03	0.80	0.08	3.01	0.98	0.80
CPN	1.04	0.79	0.08	3.00	1.00	0.79
Relative error	0.01	0.012	0	0.003	0.02	0.01

The first approach requires a critical step to achieve convergence, which involves subdividing the marking trajectory into multiple phases and intermediate points. This results in multiple phases for transitioning from the region of the initial marking to the critical region in the presence of a large number of synchronizations, or in the presence of multiple regions and critical regions. On the other hand, the adaptive approach minimizes errors caused by variations in the throughput and average markings, regardless of the initial marking and the number of synchronizations. This enables it to achieve behavior identical to that of the SPN.

5 Conclusions

In this work, two approaches were studied and compared for fluidization, sufficient conditions were added to achieve identical behavior between the CPN and SPN models. The piecewise linear approach is useful when the approximation of markings is divided into several phases and the maximal firing speeds is defined as a piecewise continuous function. The adaptive approach, on the other hand, adapts all the maximal firing speeds through an adaptive controller to correct errors in throughput and marking by referring to the asymptotic stochastic average throughput and average marking to be reached. The adaptive approach was found to be better than the piecewise linear approach for obtaining average marking and throughput estimates of the SPNs. In future research, new fluid model semantics will be utilized to study the approximation of timed CPNs by partially homothetic SPN approximations, and alternative optimal models will be investigated to address the shortcomings of directly related continuous approaches concerning the SPN transition firing rates.

Author contributions All authors have participated in the conception and design, analysis and interpretation of the data, drafting of the article, or revision of it for important intellectual content, and have given their approval for the final version of the manuscript. This manuscript has not been submitted to, nor is under review at, another journal or any other publishing venue.

Declarations

Conflict of interest The authors have no affiliation with any organization that has a direct or indirect financial interest in the subject matter discussed in this manuscript.

References

Ajmone Marsan, M., & Chiola, G. (1987). On Petri nets with deterministic and exponentially distributed firing times. *Lecture notes in computer science (including subseries lecture notes in artificial intelligence and lecture notes in bioinformatics), 266 LNCS*. (pp. 132–145). https://doi.org/10.1007/3-540-18086-9_23

Akchioui, N. (2018). About the Approximation of stochastic petri nets by continuous petri nets: several regions. In *Maghrebian Journal of Pure and Applied Science* (Vol. 1). http://revues.imist.ma/?journal=mjpas&page=index

Arzola, C., Ramírez-Treviño, A., & Silva, M. (2020). On the equilibrium sets of topologically equal conflict timed continuous petri nets. *IFAC-PapersOnLine, 53*(4), 363–370. https://doi.org/10.1016/j.ifacol.2021.04.072

Benaya, N., El-Akchioui, N., & Mourabit, T. (2018). Limits of fluidification for a stochastic Petri nets by timed continuous Petri nets. In *2018 International conference on intelligent systems and computer vision, ISCV 2018*, *2018-May*. (pp. 1–7). https://doi.org/10.1109/ISACV.2018.8354065

Bobbio, A., Puliafito, A., Telek, M., & Trivedi, K. S. (1998). Recent developments in non-markovian stochastic petri nets. *Journal of Circuits, Systems and Computers, 8*(1), 119–158. https://doi.org/10.1142/S0218126698000067

Coolahan, J. E., & Roussopoulos, N. (1983). Timing requirements for time-driven systems using augmented petri nets. *IEEE Transactions on Software Engineering, 9*(5), 603–616. https://doi.org/10.1109/TSE.1983.235261

David, R. (1993). Petri nets and grafcet for specification of logic controllers. *IFAC Proceedings Volumes, 26*(2), 683–688. https://doi.org/10.1016/s1474-6670(17)49215-9

David, R., & Alla, H. (1994). Petri nets for modeling of dynamic systems. *A Survey. Automatica, 30*(2), 175–202. https://doi.org/10.1016/0005-1098(94)90024-8

del Foyo, P. M. G., & Silva, J. R. (2017). Improving the verification of real-time systems using time petri nets. *Journal of Control,*

Automation and Electrical Systems, 28(6), 774–784. https://doi.org/10.1007/s40313-017-0343-x

Desel, J., & Juhás, G. (2001). *What is a petri net? Informal answers for the informed reader* (pp. 1–25). Berlin: Springer. https://doi.org/10.1007/3-540-45541-8_1

El Akchioui, N. (2017). Fluidification of stochastic petri net by non linear timed continuous petri net. *American Journal of Embedded Systems and Applications., 5*(4), 29. https://doi.org/10.11648/j.ajesa.20170504.11

El Moumen, H., Nabil, E. A., & Zerrouk, M. H. (2023). About the reliability analysis of complex dynamical systems via fluidification: A numerical approach. *International Journal of Reliability and Safety*. https://doi.org/10.1504/ijrs.2023.10057771

El Moumen, H., Nabil, E. A., & Zerrouk, M. H. (2023). Stochastic and continuous Petri nets approximation of Markovian model. *International Journal of Modelling, Identification and Control*. https://doi.org/10.1504/ijmic.2023.10057520

El, N., & Choukrad, S. (2016). Approximations of stochastic nets by mean of continuous petri nets. *International Journal of Computer Applications, 155*(4), 26–31. https://doi.org/10.5120/ijca2016912292

El-Moumen, H., Akchioui, N. E., & Zerrouk, M. H. (2023). Limits of direct fluidification of stochastic petri nets by timed CPNs. *AIP Conference Proceedings, 2814*(1), 040012. https://doi.org/10.1063/5.0148812

Esparza, J. (1998). Lectures on petri nets I: Basic models. (Vol. 1491). https://doi.org/10.1007/3-540-65306-6

Molloy, M.K. (1981). On the Integration of Delay and Throughput Measures in Distributed Processing Models. Ph.D. Thesis, UCLA, Los Angeles, CA.

Florin, G., Fraize, C., & Natkin, S. (1991). Stochastic petri nets: Properties, applications and tools. *Microelectronics Reliability, 31*(4), 669–697. https://doi.org/10.1016/0026-2714(91)90009-V

Giua, A., & Silva, M. (2018). Petri nets and automatic control: A historical perspective. *Annual Reviews in Control, 45*, 223–239. https://doi.org/10.1016/j.arcontrol.2018.04.006

Haas, P., & Shedler, G. S. (1989). Stochastic petri net representation of discrete event simulations. In *IEEE transactions on software engineering* (Vol. 15, pp. 381–393). https://doi.org/10.1109/32.16599

Heiner, M., Lehrack, S., Gilbert, D., & Marwan, W. (2009). Extended stochastic petri nets for model-based design of wetlab experiments. *Lecture notes in computer science (including subseries lecture notes in artificial intelligence and lecture notes in bioinformatics), 5750 LNBI* (pp. 138–163). https://doi.org/10.1007/978-3-642-04186-0_7

Horton, G., Kulkarni, V. G., Nicol, D. M., Trivedi, K. S., & Ffir Rechnerstrukturen, L. (n.d.). *Fluid stochastic petri nets: Theory, applications, and solution 1*.

Júlvez, J., Recalde, L., & Silva, M. (2005). Steady-state performance evaluation of continuous mono-T-semiflow petri nets. *Automatica, 41*(4), 605–616. https://doi.org/10.1016/j.automatica.2004.11.007

Kalaiarasi, S., & Anita, A. M. (2017). Analysis of system reliability using Markov technique. *Global Journal of Pure and Applied Mathematics., 13*(9), 5265–5273.

Karamanolis, C. (1999). Book review: elements of distributed algorithms—modeling and analysis with petri nets. *IEE Proceedings-Software, 146*(2), 128. https://doi.org/10.1049/ip-sen:19990509

Kuntz, J., Thomas, P., Stan, G. B., & Barahona, M. (2021). Stationary distributions of continuous-time markov chains: A review of theory and truncation-based approximations. In *SIAM Review* (Vol. 63(1), pp. 3–64). https://doi.org/10.1137/19M1289625

Lefebvre, D., Leclercq, E., Khalij, L., Souza De Cursi, E., & El Akchioui, N. (2009). Approximation of MTS stochastic Petri nets steady state by means of continuous Petri nets: A numerical approach. *IFAC Proceedings Volumes (IFAC-PapersOnline), 3*(PART 1) (pp. 62–67). https://doi.org/10.3182/20090916-3-es-3003.00012

Lefebvre, D., Leclercq, E., El Akchioui, N., De Cursis, E. S., & Khalij, L. (2010). A geometric approach for the homothetic approximation of stochastic Petri nets. *IFAC Proceedings Volumes (IFAC-PapersOnline), 10*(Part 1) (pp. 235–240). https://doi.org/10.3182/20100830-3-de-4013.00040

Lefebvre, D., & Leclercq, E. (2012). Piecewise constant timed continuous PNs for the steady state estimation of stochastic PNs. *Discrete Event Dynamic Systems: Theory and Applications, 22*(2), 179–196. https://doi.org/10.1007/s10626-011-0114-y

Marsan, M. A. (1990). *Stochastic Petri nets: An elementary introduction* (pp. 1–29). https://doi.org/10.1007/3-540-52494-0_23

Merlin, P. M. (1974.). *University of California Irvine a study of the recoverability of computing systems a dissertation submitted in partial satisfaction of the requirements for the degree doctor of philosophy in information and computer science*.

Moumen, H. E., Akchioui, N. E., & Zerrouk, M. H. (2022). Reliability analysis by Markov model and stochastic estimator of stochastic Petri nets. *International Journal of Reliability and Safety, 16*(1/2), 110. https://doi.org/10.1504/ijrs.2022.128614

Murata, T. (1989). Petri nets: Properties, analysis and applications. *Proceedings of the IEEE, 77*(4), 541–580. https://doi.org/10.1109/5.24143

Natkin, S. (1980). Les Reseaux de Petri Stochastiques et leur Application a l'Evaluation des Systèmes Informatiques. *Thèse de Docteur Ingegneur, CNAM, Paris, France.*

Navarro-Gutiérrez, M., Ramírez-Treviño, A., & Silva, M. (2022). Dual perspectives of equilibrium throughput properties of continuous mono-T-semiflow petri nets: Firing rate and initial marking variations. *Automatica, 136*, 110074. https://doi.org/10.1016/j.automatica.2021.110074

Pinto, C. A., Farinha, J. T., & Singh, S. (2021). Contributions of petri nets to the reliability and availability of an electrical power system in a big European hospital—a case study. *WSEAS Transactions on Systems and Control, 16*, 21–42. https://doi.org/10.37394/23203.2021.16.2

Ramchandani, C. (1974). *MAC TR-120 analysis of asynchronous concurrent systems by-petri nets*.

Recalde, L., Teruel, E., & Silva, M. (1999). Autonomous continuous P/T systems. *Lecture Notes in Computer Science (Including Subseries Lecture Notes in Artificial Intelligence and Lecture Notes in Bioinformatics), 1639*, 107–126. https://doi.org/10.1007/3-540-48745-X_8

Ribeiro, G. R., Saldanha, R. R., & Maia, C. A. (2018). Analysis of decision stochastic discrete-event systems aggregating max-plus algebra and Markov chain. *Journal of Control, Automation and Electrical Systems*. https://doi.org/10.1007/s40313-018-0394-7

Rozenberg, G., & Engelfriet, J. (1998). *Elementary net systems* (pp. 12–121). https://doi.org/10.1007/3-540-65306-6_14

Seatzu, C. (2005). Discrete, continuous and hybrid petri nets, René David and Hassane Alla, Springer, Berlin, Heidelberg, 2005, ISBN 3-540-22480-7. *International Journal of Robust and Nonlinear Control, 15*(14), 637–640. https://doi.org/10.1002/rnc.1029

Silva, M., & Recalde, L. (2002). Petri nets and integrality relaxations: A view of continuous petri net models. *IEEE Transactions on Systems, Man and Cybernetics Part c: Applications and Reviews, 32*(4), 314–327. https://doi.org/10.1109/TSMCC.2002.806063

Silva, M., & Recalde, L. (2004). On fluidification of petri nets: From discrete to hybrid and continuous models. *Annual Reviews in Control, 28*(2), 253–266. https://doi.org/10.1016/j.arcontrol.2004.05.002

Symons, F. J. W. (1980). Introduction to numerical petri nets, a general graphical model of concurrent processing systems. *ATR, Australian Telecommunication Research, 14*(1), 28–33.

Vazquez, C. R., & Silva, M. (2009). Hybrid approximations of Markovian Petri nets. *IFAC Proceedings Volumes (IFAC-PapersOnline),*

3(PART 1) (pp. 56–61). https://doi.org/10.3182/20090916-3-es-3003.00011

Vázquez, C. R., Recalde, L., & Silva, M. (2008). Stochastic continuous-state approximation of markovian petri net systems. *Proceedings of the IEEE Conference on Decision and Control*. https://doi.org/10.1109/CDC.2008.4739075

Vazquez, C. R., & Silva, M. (2015). Stochastic hybrid approximations of Markovian petri nets. *IEEE Transactions on Systems, Man, and Cybernetics: Systems, 45*(9), 1231–1244. https://doi.org/10.1109/TSMC.2014.2387097

Vázquez-Serrano, J. I., Peimbert-García, R. E., & Cárdenas-Barrón, L. E. (2021). Discrete-event simulation modeling in healthcare: A comprehensive review. *International Journal of Environmental Research and Public Health., 18*(22), 12262. https://doi.org/10.3390/ijerph182212262

Zhu, J. J., & Denton, R. T. (1988). Timed Petri nets and their application to communication protocol specification. *Proceedings-IEEE Military Communications Conference, 1*, 195–199. https://doi.org/10.1109/milcom.1988.13390